

Modification and Characterisation of Materials by Swift Heavy Ions

D.K. Avasthi

Inter University Accelerator Centre, Post Box 10502, Aruna Asaf Ali Marg, New Delhi-110 067

ABSTRACT

Swift heavy ions (SHI) available with 15 million Volt Pelletron accelerator at Inter University Accelerator Centre (IUAC) Delhi, formerly known as Nuclear Science Centre, (NSC), provide a unique opportunity to researchers for accelerator based materials science research. The major research areas can be broadly categorised as electronic sputtering, interface modifications, synthesis and modification of nanostructures, phase transitions and ion beam-induced epitaxial crystallisation. In general, SHI irradiation based-materials may not be economically feasible, still it could be of interest for very specific cases in defence and space research. The paper gives a glimpse of the current research activities in materials science with SHIs, at IUAC.

Keywords: Swift heavy ions, SHI, materials science, materials research synthesis of materials, characterisation of materials, nuclear energy loss, ion energy loss, electronic energy-loss-defects in materials, defect engineering

1. INTRODUCTION

The ions with energy ranging from a fraction of keV to GeV are useful in synthesis, modification and characterization of materials. The energetic ions during their passage through a material lose energy via two processes. These are nuclear energy loss S_n and electronic energy loss S_e . In the former process, the energy is lost by elastic collisions of incident ions with the atoms in the material, which is dominant at low energies. In the electronic energy loss process, dominant at high energies (>1 MeV/nucleon), the energy is lost by inelastic collisions of the ion with the atoms, leading to excitation or ionisation of the atoms. At these energies of heavy ions, the velocity of the ion is comparable to or higher than the velocity of Bohr electron. The ions with such high energies are also referred to as Swift Heavy Ions (SHI). The electronic energy loss for SHI is, generally, about two orders of magnitude higher than the nuclear energy loss¹. An interesting characteristic of the SHI is that it creates a columnar type of defect along its path (called as ion track), specially, in insulators. SHI during its passage through material can cause defect annealing, cluster of point defects and columnar type of defects depending on the mass and energy of the ion and the material. Therefore the SHI can be used for engineering the defects in the materials. The parameters of ion beam, which play crucial role in defect engineering, are the energy deposited per unit length and the fluence.

The ion mass and its energy, decide the magnitudes of the electronic as well as nuclear energy losses. Especially for heavy ions at high energies (*i.e.*, for SHI), the electronic energy loss decides the type of defects as the nuclear energy loss. The other ion beam parameter, fluence, dictates the number of defects (produced). The number of ion

tracks/cm² is the same as that of fluence (ions/cm²) because each ion creates an ion track. Modifications produced by SHI^{2,3} are quite different from that of low energy ions. There is a threshold of electronic energy loss, beyond which the creation of columnar defect or the latent track occurs in the materials. This threshold energy varies from material to material. It can be up to about a few hundred eV/Å for polymers and other insulators and it can be a few keV/Å for metals. There are certain materials like *Cu, Ag, Si* etc, in which track formation is not possible at any energy with monoatomic ion beams. The high energy accelerator facility at IUAC, Delhi, is a unique tool to create columnar defects and study their applications in different fields.

Another application of SHIs, is material characterisation using the technique of Elastic Recoil and Detection Analysis (ERDA). Necessary detector developments have been carried out at IUAC for ERDA, which has also been effectively utilised for sample characterisation and some online experiments.

A cutaway view of the accelerator and experimental facilities is given in Fig. 1. A view of the experimental facilities in beam hall I is given in Fig. 2.

2. ROLE OF SHI IN SYNTHESIS, MATERIAL MODIFICATIONS, CHARACTERISATION

As mentioned earlier, energetic ions, SHI in particular, play a major role in synthesis, material modifications, and characterisation as shown in Fig. 3. There are possibilities of using SHI irradiations for applications but the economic feasibility is a limiting factor. However in the areas such as defence and space, where the cost is not a determining factor, the ion beam remains viable and economically feasible. For example, the integrated circuit (IC) chip, memory chips

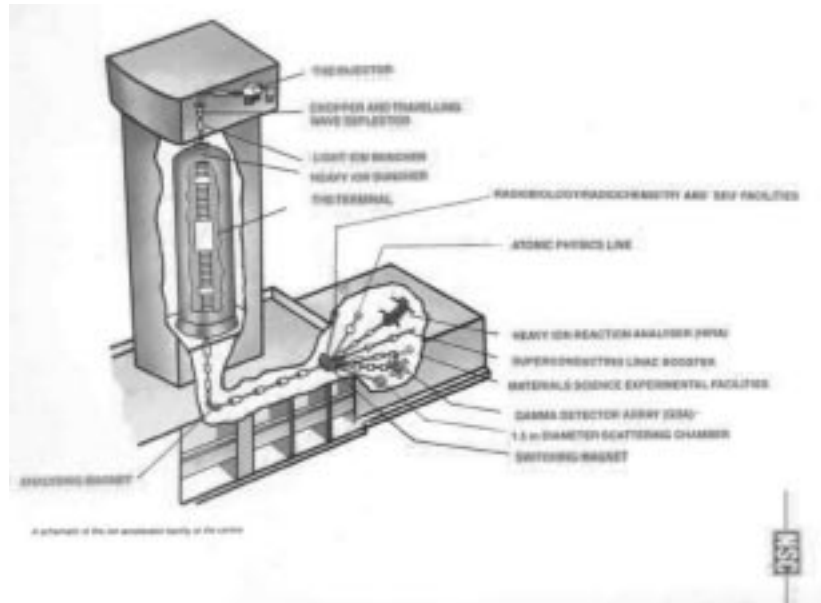


Figure 1. A cutaway view of the accelerator and experimental beam lines.

etc, can fail in the space vehicle due to space radiation. Such IC chips can be tested for their radiation hardness by the ion beams. These test experiments are carried out by the scientists of Indian Space Research Organization, (ISRO) Bangalore, at IUAC Delhi. There are a number of areas where research with SHI is undertaken at IUAC. Broadly, these can be divided in the following sections, which are discussed in brief with the examples of research performed.

- Interface modifications / Ion beam mixing
- Electronic sputtering and surface modifications
- Synthesis and modification of nano particles
- Phase transformations
- Ion beam induced epitaxial crystallization
- Development of ion beam characterization tools and on-line measurements



Figure 2. A photograph of materials science beam line.

2.1 Ion Beam Mixing

Ion beam mixing (IBM) is a process, in which the atoms of two different species across an interface are mingled together under the influence of the passage of ion beam. Conventionally it is achieved by low energy ion up to a few MeV^{7,8}. The processes involved in the ion beam mixing at low energies are the elastic collisions and subsequent collision cascades, recoil implantation, and radiation-enhanced diffusion. The collision cascade is initiated only in the case when the recoils have sufficient energy to displace the lattice atoms. The heavier ions will have large number of collision cascades as compared to that of lighter ions. IBM was considered to be a phenomenon associated with low energy ion irradiation. However since early 1990's, the ion beam mixing by SHI was observed and it attracted the attention of a few research groups,

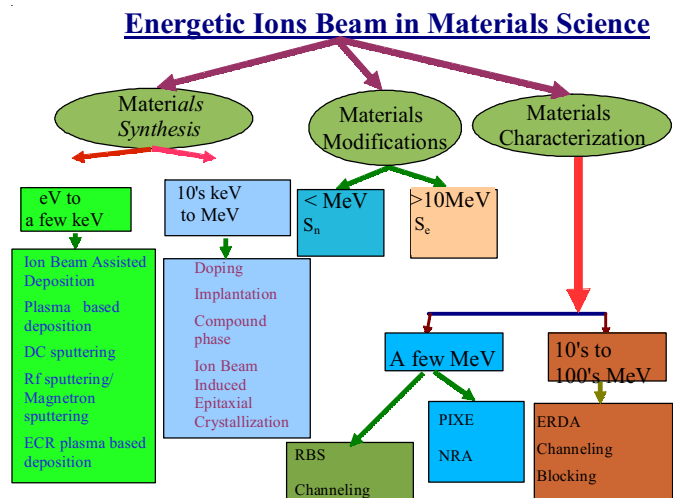


Figure 3. Sketch showing the role of ion beams in synthesis, modification and characterisation of materials.

including that of at IUAC. SHI induced mixing in several systems, e.g., Fe/Si^{9-11} , C/Si^{12} , C_{60}/Si^{13} , Co/Si^{14-15} , V/Si^{16} , Zr/Si^{17} , Cu/Ge^{18} , Ni/Si^{19} , Pt/C , Ni/C^{20} , Fe/Cr^{21} , Ni/Ge^{22} , Mn/Si^{23} , Al/Sb^{24} , Fe/Au , Fe/Ag^{25} , V , Fe , Co/Si^{26} , Ti/Au , Ti/Fe^{27} and some multilayers Fe/Tb , Fe/Ni etc²⁸⁻³⁰ have been studied at IUAC. In all the above studies, SHI induced mixing at the interface has been identified as diffusion in melt phase created by transient temperature spike^{11,16}. It is proposed that each ion produces a transient molten cylindrical zone in the material for typical time duration in the regime of picoseconds. The interdiffusion across the interface takes place during the molten phase resulting in mixing. Quantitatively, it has been shown that the diffusivity of the atomic species across the interface during the transient melt phase as obtained in these experiments^{11,16}, is of the order of 10^{-6} to 10^{-9} $m^2 s^{-1}$. Such a high diffusivity is possible only for the liquids, which supports the hypothesis that the ion beam mixing is a consequence of inter-diffusion across the interface during transient melt phase. The mixing induced by swift heavy ion at the interface of fullerene/ Si multilayer resulted in the formation of silicon carbide, which was evident by X-ray diffraction as shown in Fig. 4. Ion beam mixing in this system too is explained by interdiffusion at the interface during transient melt phase.

On the basis of experiments in several systems, Bolse³¹ *et al.* suggested the ion beam mixing takes place when the electronic energy deposition, S_e , exceeds the threshold for track creation in both the materials across the interface. It implies that IBM occurs when both the materials are in molten phase transiently as a result of the passage of ion across the interface. However it was observed that the IBM takes place, even if, the S_e threshold is overcome in one of the two materials at the interface like in Fe/Si , where it is known that track creation does not take place

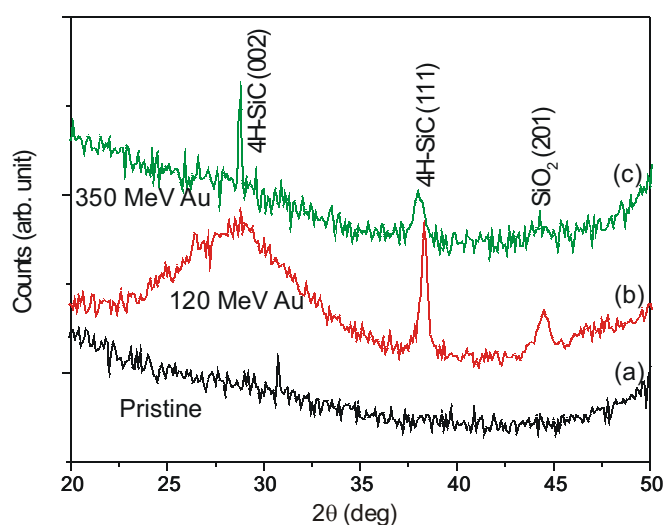


Figure 4. Formation of SiC by SHI-induced ion beam mixing in Si/C_{60} multilayer, evident by X-ray diffraction. SHI-irradiated film shows diffraction peaks corresponding to SiC .

in Si , even by GeV energy of monoatomic ion and the track creation occurs in the Fe beyond certain threshold of Se . IBM in such a case is explained³² on the basis that although bulk Si does not go to molten state, still a thin layer of Si at the interface melts transiently because its melting point is lower than that of Fe and the thermal energy transfer takes place from the Fe layer to adjacent Si , which is at lower temperature. This is shown by a schematic in Fig. 5, where a thin layer of Si undergoes a transient molten state due to thermal energy transfer of molten Fe layer. It may be noted that the increase in temperature in localised region around the ion path in Si is smaller than that in Fe as predicted by thermal spike model. Such a possibility is shown theoretically³² in Ni/Ti bilayer system, in agreement with experimental results.

It is seen that the IBM in immiscible system is either insignificant or non-existent. On contrary there are evidences of significant interface smoothing^{20,25} in specific cases. This will have direct implication in applications where the interface smoothing is desirable such as in the optical and magnetic multilayers.

The mixing has been observed by post-irradiation annealing in certain systems like Ge/Au^{18} and Co/Si^{14} . Experiments carried out using Rutherford Backscattering spectrometry did not show any mixing at the interface at fluence of 10^{13} ions/cm². The same experiments carried out following annealing of the irradiated samples showed complete mixing. Annealing of the pristine samples under similar conditions did not show this behaviour. It shows that irradiation by SHI created defects, which during annealing result in the inter-diffusion across the interface.

The ion beam-mixing has been discussed in details by S.K. Srivastava¹⁰.

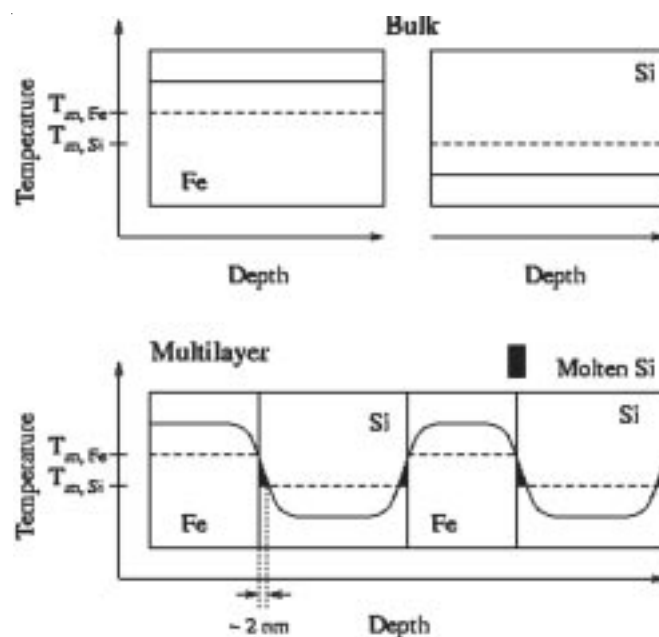


Figure 5. Schematic of the ion beam mixing showing molten Si , only at the interface, whereas Fe melts in the whole thickness of the film within ion track.

2.3 Electronic Sputtering

Sputtering is a process where the atoms from the surface and near surface region are ejected when ion beam impinges on it. Sputtering at low energies, referred to, as conventional sputtering, is dependent on nuclear energy loss and is explainable in the framework of Sigmund's theory³³. Due to S_n dependence, it is expected that the sputtering should not occur at high energies where S_n is negligible. However it has been observed that the sputtering (also) takes place at high energies beyond certain threshold of electronic energy loss. This is termed as electronic sputtering and this too has interesting applications like for the determination of the mass of extremely large molecules such as protein, bio-molecules etc.

Large molecules are sputtered by electronic excitation and the mass is measured by time of flight (TOF) technique³⁴. Large molecules such as peptides can be sputtered by electronic excitation in large numbers and the sputtered molecules are detected in the TOF set up, as discussed by Johnson and Sundqvist³⁴.

Basically there are two approaches to measure the electronic sputtering (yield). First one is to collect the sputtered species by catcher foils and quantify the corresponding yields using suitable analytical tools like Rutherford Backscattering (RBS), X-ray Fluorescence (XRF), etc. One can measure the number of sputtered atoms by TOF or quadrupole mass spectrometer. The second method measures the number of atoms left behind in thin film or measure the film thickness at the ion beam spot. The author has utilised the second method and used an indigenously developed gaseous telescope detector at IUAC for these measurements. There have been several experiments on electronic sputtering using the online ERDA facility. The experiments showed that the electronic sputtering is dependent on; (i) film thickness³⁵ (ii) grain size³⁶ (iii) phase³⁷ etc. Measurements of electronic sputtering from different allotropes of C were performed, exhibiting a trend in variation of electronic sputtering. These experimental results of electronic sputtering measurements were explainable under thermal spike model.

Recently, detailed experiments³⁸ were performed on the electronic sputtering of LiF by online ERDA. The LiF thin films of different grain size and different thickness were specially prepared to study the effects of thickness and grain size on the electronic sputtering, as shown in Fig. 6. It was concluded that the electronic sputtering depends both on the grain size and the film thickness. The scattering of electrons (produced during the passage of ions) from the surface and interface of thin film as well as from the grain boundaries causes the confinement of electrons within thin film^{35,39}. It results in higher temperature spike and its duration in thinner films and the atoms from the surface escape from the film during this temperature spike, and thus, sputtering mediated by electronic excitation occurs. Since thinner film has higher temperature spike and its duration, therefore thinner films give higher electronic sputtering yield. Similar argument is given for the higher

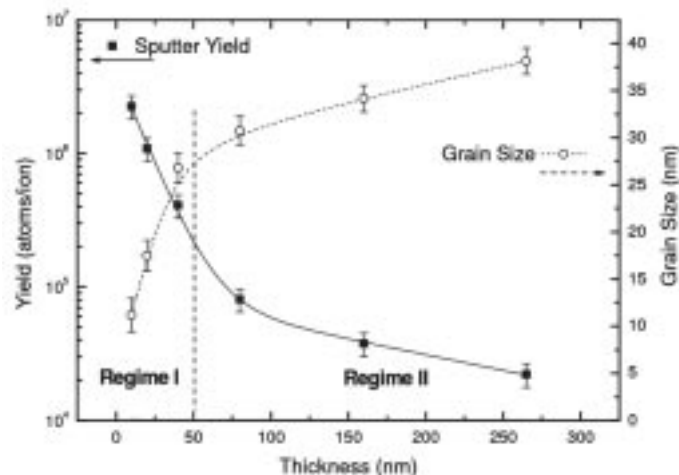


Figure 6. Plots for the variation of grain size with film thickness of LiF and the variation of sputtering yield with film thickness of LiF under 120 MeV Ag ion irradiation.

sputtering rate as observed in films having smaller grain size. In a similar way unexpectedly, high sputtering yield was observed in thin Au films under SHI impingement, increasing with decrease in film thickness⁴⁰. This was also explained in the framework of thermal spike and confinement of electrons due to the scattering from surface and interface. The electronic sputtering has been discussed in details by S. Ghosh³⁷.

2.4 Swift Heavy Ions in Nano Structuring

Nanotechnology has become very popular and attracting field of research due to the possibilities of a wide range of promising futuristic applications. Physicists find it interesting as the nanoparticles represent a picture of quantum mechanically confined potential, where the confining dimension is represented by the size of nanoparticles. The ability of altering the properties (physical, electronic, optical, etc.) by merely changing the size of the nano-particles makes it extremely suitable for a large variety of applications.

In the field of nano materials, the energetic ions are of use for (suggested addition: both synthesis and modification. The important issues in nano materials are the (i) control of the size of particles (ii) the size distribution and (iii) altering the shape of particles. Ion beams play a significant role related to all these issues. Some of the research works carried out at IUAC are cited here.

2.5 Nano Phase Generation by SHI

2.5.1 Generation of C nanowire Like Structures

The unique feature of SHI of creating ion tracks (typically of dia up to 10 nm) provides a tool to create nanowire type of structures as demonstrated and discussed here.

In experiments involving SHI irradiation of Si-based polymers, carried out in collaboration with a French group, it was shown⁴¹ that the C clusters all along the ion track in the entire sub-micron thick film can be created. The cylinders were however filled only up to 60 per cent or

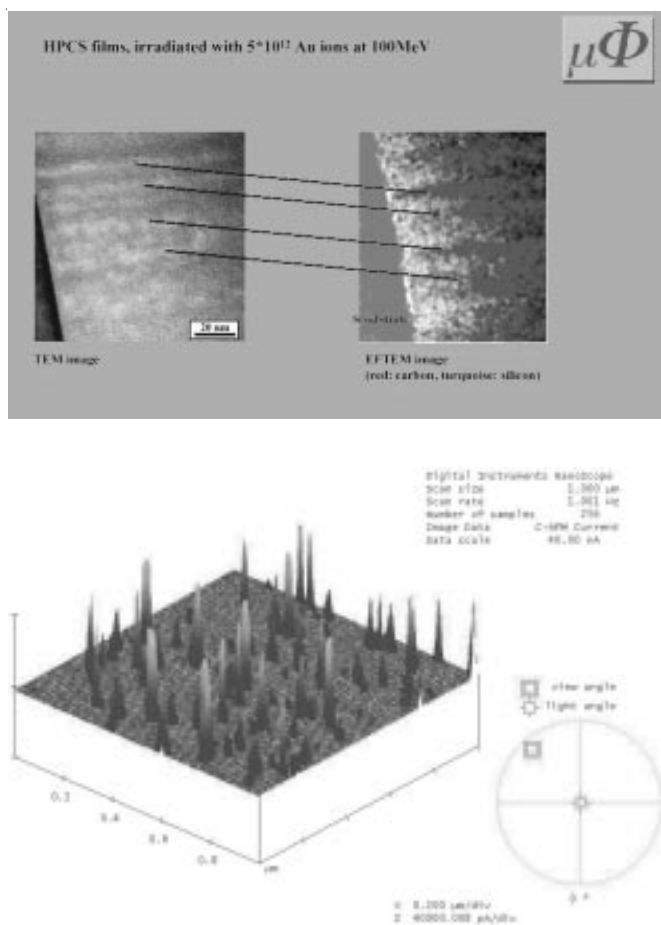


Figure 7. (a) TEM and EFTEM picture of 100 MeV *Au* ion irradiated anhydro polycarbo silane and (b) Conducting C tracks in 120 MeV *Au* ion irradiated fullerene thin film as evident by conducting atomic force microscopy.

so with the clusters. If this filling can be increased to 100 per cent, it will be like a quantum wire. In yet another study, polycarbosilane (PCS) and Allylhydridopolycarbosilane (HPCS) films were irradiated by 100 MeV *Au* ions. Transmission electron microscopy (TEM) and Energy filter TEM revealed the alignment of carbon clusters all along the ion path as shown in Fig. 7 (a), looking like carbon nanowire. The densification of C clusters in the ion track has been explained by diffusion within track during the transient melt phase⁴². It is shown by online ERDA that hydrogen is lost within a cylindrical diameter along the beam direction. The diameter of the cylindrical region, from where the hydrogen is released, matches well with the track diameter within which the C clusters are formed.

SHI irradiation of fullerene film leads to an increase in conductivity. It is therefore expected that all along each ion track (of diameters of ~10 nm or so) created by individual ion passage will have higher conductivity than the surrounding. It is therefore possible to generate conducting C nanorods or nanowires in the fullerene matrix by high energy heavy ion irradiation, which has been demonstrated recently at IUAC⁴³. Fig. 7 (b) shows results obtained using

conducting Atomic Force Microscopy on such samples. The conductivity of ion track zone has been observed to be several orders of magnitude higher than that of the pristine surrounding region. The observed diameter of the conducting tracks is found to be 40 nm to 60 nm which is larger than the expected ion track diameter. This was attributed to the formation of fullerene dimers in the annular cylindrical region around the ion track and subsequent lateral percolating conduction. The field emission properties of these conducting nanowires were also undertaken⁴⁴.

2.5.2 SHI Induced Formation of Semiconducting Nanoparticles

Thin films of *SiO_x* were irradiated with swift heavy ions⁴⁵, resulting in formation of *Si* nanocrystals in the film. This was investigated by PL and TEM. The irradiation may cause evolution of oxygen from the film. Therefore possible reaction due to SHI was formation of *Si* nano crystal with *SiO₂* accompanied with release of oxygen. Thus, swift heavy ion produces an action similar to the reduction process in *SiO_x* matrix, resulting in formation of *Si* nanoparticles. Similar experiments of irradiation of *GeO_x* and *Ge* in silica matrix resulted in precipitation of *Ge* nanoparticles in respective matrices⁴⁶. The formation of *Si* and *Ge* nanoparticles by the ion irradiation of *SiO_x* and *GeO_x* respectively could be considered as ion beam induced reduction process. In principle, the reduction process can be achieved by annealing the sample in reducing environment (95% *Ar* and 5% *H₂*). However the advantage of ion beam is the spatial selectivity.

2.6 Influence of SHI on Nanoparticles

2.6.1 Effect of SHI Irradiation on Metal Particles in Insulating Matrix

Metal nano-particles in an insulating transparent matrix like silica have the property of absorbing visible light in a narrow band owing to surface plasmon resonance. The collective motion of free electrons in the particle induced by the oscillating electric vector of the incident electromagnetic wave, is known as surface plasmons. The resonance frequency of the spherical shape metal nano-particles depends on the size of the particle and the dielectric constants of the particle and the surrounding medium. In such cases of metal nano-particles in an insulating transparent matrix, the UV-Vis spectroscopy becomes an excellent tool to characterise the nano-particles by surface plasmon resonance, evident by absorption in visible region.

The effect of SHI on metal nano-particles is of interest to

- (i) understand the interaction of energetic ions with low dimension matter
- (ii) to look into the details of modification to probe the possibilities of engineering the nano structures.

It can be seen from the following discussion that the ion track size and the the parameters of nanocomposite such as behaviour of matrix under ion beam in terms of track creation, particle size, metal fraction, etc. decide the

effect of ion beam on altering the shape and size of the embedded nanoparticles.

2.6.2 Change of Size and Shape Under SHI Irradiation

The samples of *Au*-teflon nanocomposite on TEM grids were irradiated by 100 MeV *Au* ion beam at different fluences. Size of *Au* particles was not spherical in the pristine films as investigated by TEM. After irradiation it was noticed⁴⁷ that the particles coalesced together to form bigger and spherical particles under SHI irradiation. Similarly the growth of *Au* particles (from 4 nm to 9 nm) in silica matrix (19.6 at.% *Au* in silica) was also observed under 90 MeV *Ni* ion irradiation. It was investigated⁴⁸, using the recently installed *in situ* XRD facility in the materials science beam line. The XRD spectra recorded *in situ* in the experiment of the irradiated sample are shown in Fig. 8. A photograph of the *in situ* XRD facility is shown in Fig. 9. The reduction in size of *Au* particles (buried in silica matrix) under 90 MeV *Ni* ion irradiation was observed when the *Au* was about 5 at per cent in silica⁴⁹.

In the experiments with larger *Au* particles (>14nm) in silica matrix (obtained by annealing of the *Au*-silica nanocomposite thin film with 15 at per cent *Au*), it was observed that the particles elongate along the ion beam direction⁵⁰, under 120 MeV *Au* ion irradiation, as shown in Fig. 10. The elongation happens when the *Au* particle size is larger than the track diameter size in silica. Typical track diameter in silica is about 7 nm.

To summarize, it can be stated on the basis of several

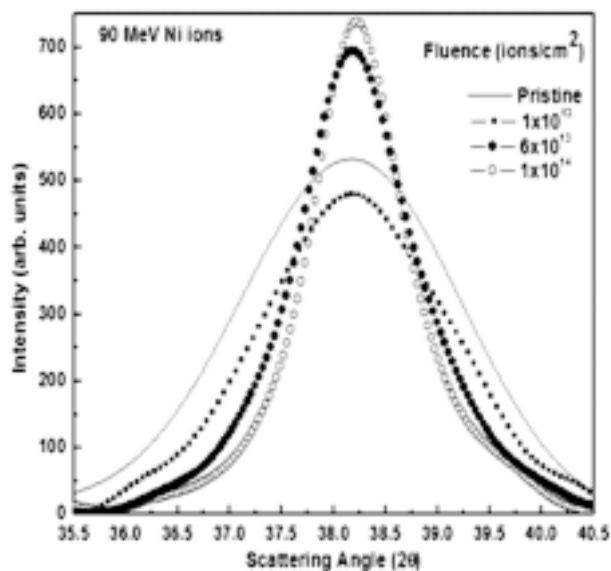


Figure 8. The X-ray diffraction pattern of *Au* silica nanocomposite thin film irradiated by 90 MeV *Ni* ions at different fluences as recorded by *in-situ* X-ray diffractometer. Since the full width at half maxima (fwhm) is inversely proportional to the average particle size, it is clear that the average particle size increases with the fluence.



Figure 9. A view of *in-situ* X-ray diffractometer in the beam line. The chamber has a port to connect to the accelerator beam line. The chamber also has two Kapton (polyimide) windows for the entry and exit of the incident and diffracted X-rays respectively.

experiments that when the *Au* nanoparticles (buried in silica thin film) are smaller than the track diameter in silica, the increase or decrease in size of particles occur depending on the metal fraction. The increase in particle size occurs when the metal fraction is high (19.6 at. per cent), whereas

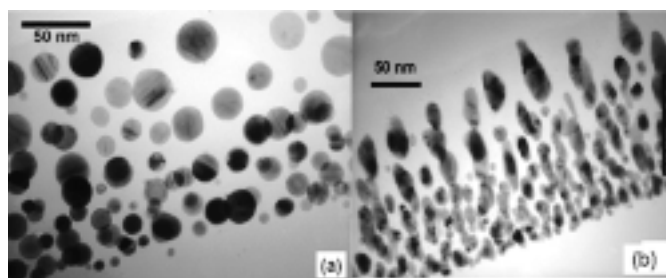


Figure 10. Dependence of electronic sputtering on the film thickness and grain size.

the decrease in particle size occurs when the metal fraction is low (5 at. per cent). When the *Au* nanoparticles are larger than the track diameter, the elongation of particles occur along the ion beam direction. These were explained on the basis of dissolution and precipitation of metal particles⁵¹ during the transient molten region within the ion track.

2.6.3 Effect of SHI Irradiation on *Ag* Particles in Insulating Matrix

Ag nano-particles embedded in teflon polymer matrix were also made by RF co-sputtering on the TEM grid and were irradiated at different fluences. Teflon matrix is used because of its higher thermal stability. TEM study of the irradiated samples indicated⁴⁷ behaviour different from that observed in case of *Au*-teflon nanocomposite thin film. The average size of particles is reduced slightly.

It appeared that there was loss of *Ag* content which was attributed to the electronic sputtering of *Ag* particles. Smaller the size of particle, greater is the confinement of electron produced in the wake of passage of incident high energy ion^{38,40}, which causes higher temperature rise resulting in transient molten state during which the atoms escape, resulting in loss of *Ag* atoms from *Ag* nanoparticles near the surface.

In another experiment, *Ag* particles were grown in silica by magnetron co-sputtering and then the response of irradiation of 100 MeV *Ag* was studied⁵². It was observed that the *Ag* atoms were released from the clusters as a result of irradiation indicating dissolution of clusters in silica. This conclusion was based on the decreasing integral intensity of the plasmon resonance peak with the fluence. The decrease in particle size in the work by Biswas, *et al*⁴⁷, is also consistent with the present observation. It is apparent that the matrix in which the particles are existing also play a role in deciding the effect of swift heavy ions on the nano particles. The elongation of *Ag* nanoparticles in silica matrix was observed under SHI irradiation in recent experiments^{53,54}, for the case when the *Ag* nanoparticles were bigger than the track diameter, similar to what is observed in the case of *Au* nanoparticles.

2.6.4 Effect of SHI on Copper Oxide Nanoparticles

The copper oxide nano-particles were prepared by activated reactive evaporation method⁵⁵. The effect of large electronic excitation (24 keV/nm) generated by the 120 MeV *Ag* ions on the copper oxide nano-grain film was examined by X-ray diffraction, Raman spectroscopy and photoluminescence⁵⁶. XRD analysis revealed that the pristine films were having both the phases *CuO* and *Cu₂O* and the irradiation induced a phase change from *CuO* to *Cu₂O*. The ion beam irradiation thus have the effect similar to the reduction process as seen in the case of formation of *Si* nanoparticles in Section 3.4.1.2. It is most likely due to release of oxygen. The crystalline quality of the films appeared to have improved with irradiation. It was observed that the PL intensity increased in the irradiated sample, which was attributed to the removal of surface states.

2.6.5 Effect of SHI on Semiconductor Nanoparticles in Polymer Matrix

Nano-particles of *Zn* in polyvinyl alcohol matrix were prepared and irradiated by 100 MeV *Cl* ions. It was observed⁵⁷ that the particle size increased from about 1 nm for pristine sample to 4 nm at the fluence of 5×10^{12} ions/cm². The size went up sharply at the fluence of 10^{13} ions/cm². The characterisations were performed by UV-Vis absorption spectroscopy and electron microscopy.

3. PHASE TRANSITIONS BY SHI

SHI during its passage through the material creates a transiently molten cylindrical zone along its path, during a temperature spike of the time duration of the order of picosecond. The molten zone due to larger volume than

its original volume, causes pressure to its surrounding. Thus, the material within this cylindrical region and/or the surrounding may experience very high pressure leading to a phase transition.

3.1 Modifications in Diamond Like Carbon (DLC) and Fullerene Thin Films

There have been several studies on SHI-induced phase transformations in allotrope of carbon. A good diamond thin film is hardly affected by SHI irradiation whereas a fullerene film transforms to an amorphous carbon (state) under SHI irradiation. The formation of dimers and trimers of fullerene also referred to as polymerisation of Fullerene^{58,59} has also been observed at low fluences of swift heavy ions. It is postulated that the annular cylindrical region surrounding the ion path, has such temperature and pressure conditions that favour transition from fullerene to its dimer or polymer, as shown in the schematic in Fig. 11. The band gap of the irradiated film decreases drastically with fluence⁵⁸. The changes in the DLC type of films depend on its initial D and G bands intensities and widths. *H* and *C* as well as alone in several DLC films from different research groups have been measured to provide an input to understand the properties of the films^{60,61} and growth mechanism.

Exotic structures like *Ni* inside Carbon nanotube (CNT) have been of interest and the stability of these with ion beam have been studied at IUAC^{62,63}. It is observed that the multi-wall CNTs with larger number of walls are resistant to damage by ion irradiation, whereas the CNTs with smaller number of walls are prone to damage⁶². *Ni* being in nano dimension gets affected by the swift heavy ion irradiation

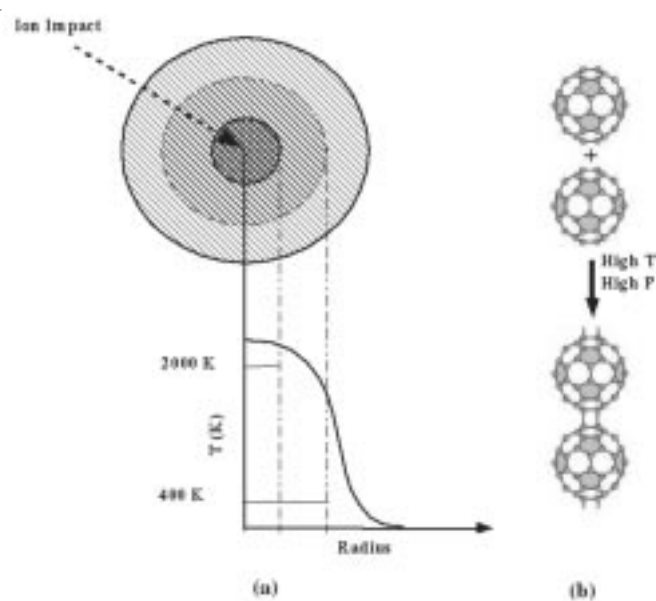


Figure 11. Schematic of the annular cylindrical region surrounding the ion path, has such temperature and pressure conditions that favour transition from fullerene to its dimer or polymer

in terms of the lattice distortions⁶³ whereas the bulk *Ni* is known to be not affected by SHI irradiation.

3.2 Modification in Oxide Materials by SHI

There have been several SHI irradiation studies on different type of oxide films like high Tc superconducting (HTS) thin films ($Y_1Ba_2Cu_3O_{7-x}$, $Bi_2Sr_2Ca_4O$), ferrite films, $La_{0.25}Ca_{0.75}MnO_3$ (LCMO) films, etc. The magnetic lines of force are repelled by HTS material thin films. The magnetic flux lines have current loops associated with them which are referred as vortices, which pose hindrance in the flow of charge carriers. The vortices can lead to destruction of superconductivity. These vortices can be pinned by defects. The columnar defects can therefore provide a mean for pinning the flux⁶⁴, a very useful aspect in practical applications. Favorable changes in transition temperature have been observed in the irradiated LCMO, which are likely due to the pressure exerted by the material in the ion track to its surrounding⁶⁵. AFM study of the irradiated sample gave an indication of such pressure surrounding the ion impact point. The dissolution of *Co* clusters buried in *ZnO* (obtained by implantation of *Co* in *ZnO*) was achieved⁶⁶ by irradiation of swift heavy ions. The dissolution of *Co* clusters is considered to be of great significance from the point of view of dilute magnetic semiconductors.

4. ION BEAM INDUCED EPITAXIAL CRYSTALLISATION

The synthesis of a thin crystalline *Si* layer on (an) insulating layer is of technological importance for devices. Ion beam is a unique tool in achieving it at relatively lower temperatures. Irradiation of *Si* by low energy (typically 100 to 400 keV) Oxygen or Nitrogen ions irradiation gives an insulating oxide or nitride layer near the surface region of *Si* substrate, at a typical depth of 200 nm. to 500 nm. The ions (nitrogen or oxygen) during their passage before coming to rest, amorphize the region they traverse. Thus, one achieves a layer of amorphous *Si* on the insulating oxide or nitride layer. The conversion of the top amorphous *Si* layer to crystalline *Si* can be achieved at high temperatures above 1000 °C. Such a high temperature annealing for recrystallisation is undesirable in processing of materials. Ion beam gives a better alternative for converting the amorphous *Si* to crystalline *Si* by irradiation at temperatures up to a few hundred degree centigrade. Low-energy irradiation upto a few MeV has been exploited⁶⁷ for the recrystallisation process. In this energy region, either the nuclear energy loss dominates or both the electronic and nuclear energy loss are of comparable value. At IUAC, the recrystallisation process by electronic energy deposition is under investigation and has yielded interesting results. Degree of crystallisation is studied by RBS channeling and TEM experiments. It has been shown that the swift heavy ion-induced epitaxial crystallisation can be achieved by irradiation at 300 °C to 400 °C^{68,69}. It was concluded from several experiments at IUAC that swift heavy ion beam induced crystallisation

strongly depends⁷⁰ on the the ratio of S_e to S_n of the ion beam used as shown in Fig. 12.

5. DEVELOPMENT OF ION BEAM CHARACTERISATION TOOLS AND ONLINE MEASUREMENTS

One of the unique features of SHI is the characterisation of materials by ERDA. Suitable gaseous-based telescope detector were developed at IUAC, New Delhi, for characterisation by ERDA⁶. These have also been effectively utilised for online monitoring of electronic sputtering and ion beam mixing induced by swift heavy ions. The schematic diagram of a large area position sensitive detectors developed at IUAC is shown in Fig. 13(a). Necessary electronics for signal processing and gas-handling system [Fig. 13(b)], is integrated with the irradiation chamber in beam lines of Pelletron and superconducting linear accelerator. Large area has an advantage of faster data acquisition and therefore taking short time in collecting data with reasonable statistics. But it suffers with the poor depth resolution due to kinematic broadening. The problem of kinematic broadening is overcome using the position sensitive feature(s) built in the detector so that the correction for kinematic broadening can be implemented by software. These telescope detectors with ERDA have been effectively utilized^{38,71,72} for online studies of electronic sputtering and ion beam mixing. Typical recoil spectra are shown in Fig. 14 which allowed to determine the electronic sputtering of *LiF*. We proposed that the recoils produced by incident ion provide information on quantity of that particular element and depth distribution whereas each ion producing track (if incident ion energy is greater than threshold for creation track) may cause sputtering from the surface and mixing at the interface. Thus incident ions play dual role of pump and probe as shown in Fig. 15 and this become as online monitoring of ion-induced modifications at the surface and the interface.

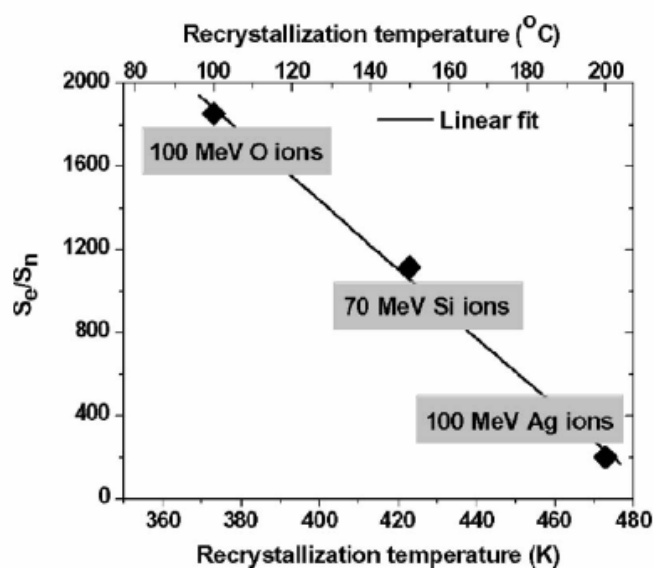
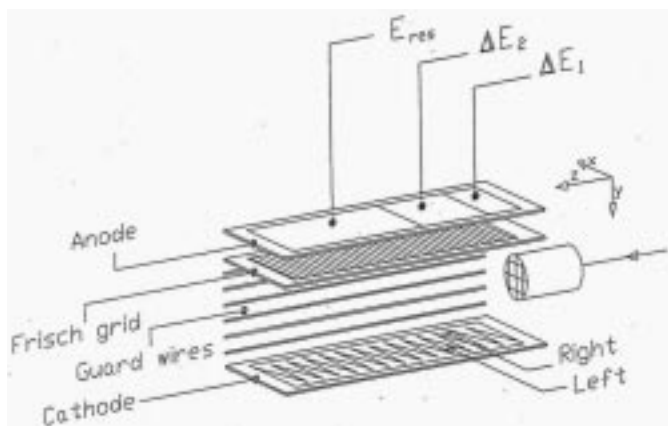
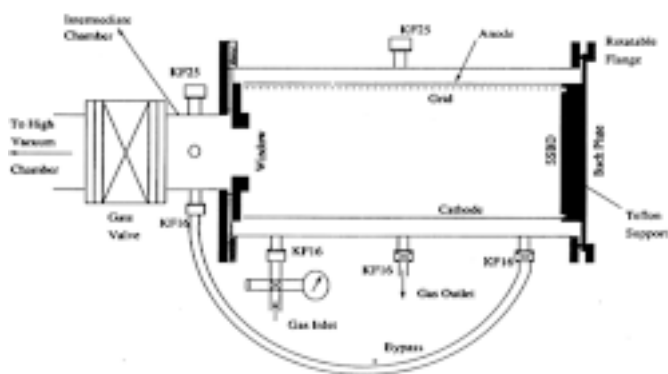


Figure 12. Dependence of ion beam induced epitaxial crystallisation on the ratio of S_e/S_n .



(a)



SECTIONAL VIEW OF THE POSITION SENSITIVE E-E TELESCOPE DETECTOR

(b)

Figure 13. (a) A schematic of the gaseous telescope detector indigenously designed fabricated and installed in two beam lines. The upper and lower plates are anode and cathode with a semiconductor detector at the back where the lighter recoils finally get stopped and (b) The schematic of gas handling set up for the telescope detector. The detector is connected to the irradiation chamber through the gate valve.

Details of the research programs and experimental facilities are available on the website www.iuac.ernet.in.

ACKNOWLEDGEMENTS

The author thanks the vision of Prof G.K. Mehta for initiation of the work in the field of materials science with ion beam at IUAC Delhi. He owes thanks to Dr Amit Roy, Director of IUAC for continuous encouragement. He is also thankful to Department of Science and Technology, New Delhi, for financial support under the project ‘Intensifying Research in High Priority Areas’. The developments of the experimental facilities deserve appreciation of A. Tripathi, R. Kumar, F. Singh, Shivakumar, S.A. Khan, P.K. Kulriya, I. Sunaliya, R.N. Dutta, D. Kanjilal, D. Kabiraj, S.R. Abhilash, P. Barua, A. Kothari and R. Ahuja. There have been several joint research programs with foreign universities in Germany (Munich, Stuttgart, Kiel, Darmstadt, HMI Berlin), France (Orsay, Caen), Italy (Padova), USA (Maryland), Korea and Singapore.

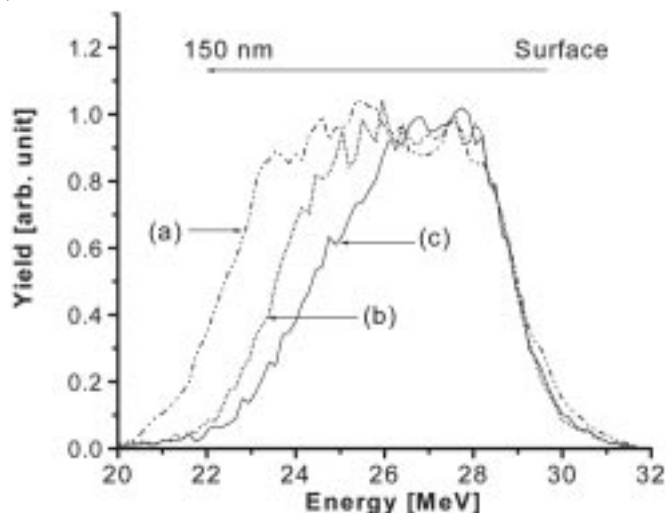


Figure 14. Recoil spectra of thin LiF film at different fluences of 120 MeV Ag ions, showing the decrease in film thickness with fluence.

Energy Loss: Slowing down of ion (dE/dx)

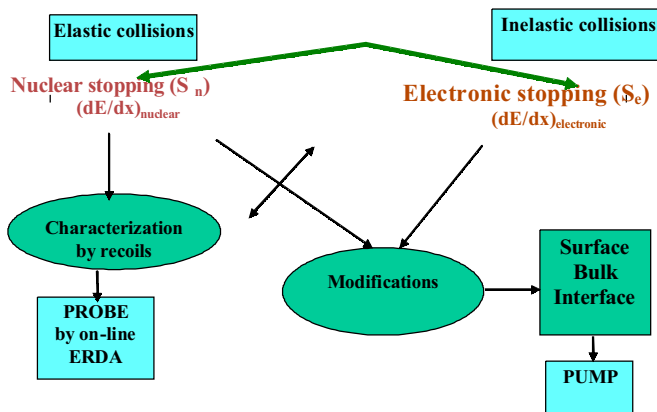


Figure 15. Schematic showing two energy loss processes and the philosophy of online monitoring of the ion-induced modifications by recoils.

REFERENCES

1. Ziegler, J.F.; *et al.* Stopping and Ranges of Ions in Matter, Pergamon, New York, 1985.
2. Kanjilal, D. Swift heavy ion-induced modification and track formation in materials, *Current Science* 2001, **80**, 1560-1565
3. Avasthi, D.K. ; Some interesting aspects of swift heavy ions in materials science, *Current Science* 2000, **78**, 1297-1303
4. Asokan, K & Roy, A. Nuclear Science Centre: A profile, *Nucl. Phys. News*, 2003, **13**, 4-10.
5. Avasthi, D.K.; Kabiraj, D.; Bhagwat, A.; Mehta, G. K.; Vankar, V. D. & Ogale, S. B. Simultaneous detection of light elements by ERDA with gas-ionisation/Si $\bar{A}E$ -E detector telescope, *Nucl. Instr. and Meth. B* 1994, **93**, 480-84.
6. Avasthi, D.K. & Assmann, W. ERDA with swift heavy

- ions for materials characterization, *Current Science* 2001, **80**, 1532-1541.
7. Mayer, J.W.; Tsaur, B. Y.; Lau, S. S. & Hung, L.S. Ion-beam-induced reactions in metal-semiconductor and metal-metal thin film structures, *Nucl. Instr. and Meth. B* 2001, **182/183**, 1-13.
 8. Santos, D.L.; de Souza, J. P.; Amaral, L. & Boudinov, H. Ion beam mixing of *Fe* thin film and *Si* substrate, *Nucl. Instr. and Meth. B* 1995, **103**, 56-59.
 9. Assman, W.; Dobler, M.; Avasthi, D. K.; Kruijjer, S.; Mieskes, H. D. & Nolte, H. Swift heavy ion induced formation of α -*FeSi*₂, *Nucl. Instr. and Meth. B* 1998, **146**, 271-277.
 10. Srivastava, S.K.; Ghosh, S.; Gupta, A.; Ganesan, V.; Assman, W.; Kruijjer, S. & Avasthi, D. K. Conversion Electron Mössbauer Study of Mixing Induced by Swift Heavy Ions at the *Fe/Si* Interface, *Hyperfine Interaction* 2001, **133**, 53-57.
 11. Srivastava, S.K.; Avasthi, D. K.; Assaman, W.; Wang, Z. G.; Kucal, H.; Jacquet, E.; Carstanjen, H. D. & Toulemonde, M.; Test of the hypothesis of transient molten state diffusion for swift-heavy-ion induced mixing, *Phys. Rev. B* 2005, **71**, 0193405-0193408.
 12. Asokan, K.; Srivastava, S.K.; Kabiraj, D.; Mookerjee, S.; Avasthi, D. K.; Jan, J. C.; Chiou, J. W.; Pong, W. F.; Ting, L. C. & Chien, F. Z. Study of ion beam mixing in *C/Si* multilayers by X-ray absorption spectroscopy, *Nucl. Instr. and Meth. B* 2002, **193**, 324-328.
 13. Srivastava, S.K.; Kabiraj, D.; Schattat, B.; Carstanjen, H. D. & Avasthi, D. K.; Swift heavy ion induced modification of *Si/C₆₀* multilayers, *Nucl. Instr. And Meth. B*, 2004, **219/220**, 815-819.
 14. Bhattacharya, D.; Srivastava, S.K.; Sahoo, P. K.; Principi, G.; Kabiraj, D.; Som, T.; Kulkarni, V. N.; & Avasthi, D. K. Swift heavy ion induced modification of the *Co/Si* interface; cobalt silicide formation, *Surface and Coatings Technology*, 2002, **158/159**, 59-63.
 15. Chakraborty, B.R.; Halder, S. K.; Karar, N.; Kabiraj, D. & Avasthi, D. K. Formation of cobalt silicides as a buried layer in silicon using high energy heavy ion irradiation, *J. of Phys. D: Applied Physics*, 2005, **38**, 2836-2840.
 16. Diva, K.; Kabiraj, D.; Chakraborty, B. R.; Shivaprasad, S. M. & Avasthi, D. K. Investigation of *V/Si* mixing induced by swift heavy ions, *Nucl. Instr. And Meth. B* 2004, **222**, 169-174.
 17. Sisodia, V.; Jain, R.K.; Bhattacharya, D.; Kabiraj, D. & Jain, I.P.; Structural modification by swift heavy ion at metal/*Si* interface, *Rad. Measurements*, 2003, **36**, 657-661
 18. Kumar, S.; Chauhan, R. S.; Khan, S. A.; Bolse, W. & Avasthi, D. K. Swift heavy ion induced mixing in metal/metal system, *Nucl. Instr. And Meth. B* 2006, **244**, 194-197.
 19. Sisodia, V.; Kabiraj, D. & Jain, I. P. Schottky barrier height measurement of swift heavy ion intermixed *Ni*-Silicide interface, *Nucl. Instr. And Meth. B* 2004, **225**, 256-260.
 20. Gupta, A.; Pundita, Suneel.; Avasthi, D. K.; Lodha, G. S. & Nandedkar, R. V. Swift heavy ion irradiation effects in *Pt/C* and *Ni/C* multilayers, *Nucl. Instr. And Meth. B* 1998, **146**, 265-270.
 21. Paul, A.; Gupta, Ajay .; Chaudhari, S. M .; Phase, D. M .; Ghosh, S. & Avasthi, D.K ; Swift heavy ion irradiation effects on magnetoresistance of *Fe/Cr* multilayers, *Nucl. Instr. And Meth. B* 1999, **156**, 158-161.
 22. Som, T.; Satpati, B .; Satyam, P. V.; Kabiraj, D.; Ayyub, P.; Ghosh, S.; Gupta, Ajay; Dev, B.N. & Avasthi, D. K. Swift heavy ion induced interface modification in *Ni/Ge*, *Nucl. Instr. And Meth. B* 2003, **212**, 206-210.
 23. Chaudhuri, S.; Biswas, S.; Gupta, A.; Avasthi, D. K.; Bhattacharya, D.; Teichert, S. & Sarkar, D. S. Formation of transition metal silicides by high energy ion beam mixing in *Mn/Si* and *Ni/Si* single and multilayer samples, *Nucl. Instr. And Meth. B* 2004, **217**, 589-597
 24. Mangal, R.K.; Singh, M.; Vijay, Y. K. & Avasthi, D. K. Preparation of *Al-Sb* semiconductor by swift heavy ion-irradiation, *Bull. Mater. Sci.* 2006, **29**, 653-657.
 25. Rumbolz, C.; Kumar, S.; Chauhan, R. S.; Kabiraj, D. & Avasthi, D.K. Smoothing of *Fe/Au* and *Fe/Ag* multilayers by swift heavy ion bombardment, *Nucl. Instr. And Meth. B* 2006, **245**, 145-149.
 26. Gupta, A.; Chauhan, R. S.; Agarwal, D. C.; Kumar, S.; Khan, S. A.; Tripathi, A.; Kabiraj, D.; Mohapatra, S.; Som, T. & Avasthi, D. K. Smoothing, roughening and sputtering; the complex evolution of immiscible *Fe/Bi* bilayer system, *J. Phys. D: Applied Physics* 2008, **41**, 215306(1)-215306(8)
 27. Kumar, S.; Chauhan, R.S.; Khan, S.A.; Bolse, W. & Avasthi, D.K. Swift heavy ion induced mixing in metal/metal system, *Nucl. Instr. And Meth. B* 2006, **244**, 194-197.
 28. Gupta, A.; Paul, A.; Gupta, R.; Avasthi, D.K.; Principi, G. Swift heavy ion irradiation effects on perpendicular magnetic anisotropy in *Fe/Tb* multilayers, *J. Phys. B: Condens. Matter Phys.* 1998, **10**, 9669-9673.
 29. Bhattacharya, D.; Principi, G.; Gupta, A. & Avasthi, D. K. Swift heavy ion beam mixing in *Mo/Si* system, *Nucl. Instr. And Meth. B* 2006, **244**, 198-201.
 30. Srivastava, S.; Kumar, Ravi.; Gupta, A.; Patel, R. S.; Majumdar, A. K. & Avasthi, D. K.; Swift heavy ion induced mixing in *Fe/Ni* multilayer, *Nucl. Instr. And Meth. B* 2006, **243**, 304-312
 31. Schattat, B. & Bolse, W. Fast heavy ion induced interface mixing in thin-film systems, *Nucl. Instr. And Meth. B* 2004, **225**, 105-110.
 32. Wang, Z.G.; Dufour, Ch.; Euphrasie, S. & Toulemonde, M. Electronic thermal spike effects in intermixing of bilayers induced by swift heavy ions, *Nucl. Instr. And Meth. B* 2003, **209**, 194-199.
 33. Sigmund, P. Theory of Sputtering. I. Sputtering Yield of Amorphous and Polycrystalline Targets, *Phys. Rev.* 1969, **184**, 383-416.

34. Avasthi, D.K.; Ghosh, S.; Srivastava, S.K. & Assmann, W. Existence of transient temperature spike induced by SHI: evidence by ion beam analysis, *Nucl. Instr. And Meth. B* 2004, **219/220**, 206-214.
35. Ghosh, S.; Tripathi, A.; Som, T.; Srivastava, S.K.; Ganesan, V.; Gupta, A. & Avasthi, D.K. Nitrogen evolution from copper nitride films by MeV ion impact, *Rad. Effects Defects in Solids*, 2001, **154**, 151-153.
36. Ghosh, S.; Avasthi, D. K.; Som, T.; Tripathi, A.; Kabiraj, D.; Ingale, A.; Mishra, S.; Ganesan, V.; Zhang, S. & Hong, X. Structure dependent electronic sputtering of a-C:H films by swift heavy ions, *Nucl. Instr. and Meth. B* 2002, **190**, 164-168.
37. Ghosh, S. Ph.D. Thesis 2000, Jawar Lal Nehru University, Delhi.
38. Kumar, Manvendra; Khan, S. A.; Rajput, Parasmani, Singh, F.; Tripathi, A.; Avasthi, D. K. & Pandey, A. C. Size effect on electronic sputtering of LiF thin films, *J. Appl. Phys.* 2007, **102**, 083510(1)-083510(6).
39. Gupta, A.; Pandita, S.; Avasthi, D. K.; Lodha, G. S. & Nandedkar, R. V. Swift heavy ion irradiation effects in Pt/C and Ni/C multilayers, *Nucl. Instr. and Meth. B* 1998, **146**, 265-270.
40. Gupta, A. & Avasthi, D. K. Large electronically mediated sputtering in gold films, *Phys. Rev. B* 2001, **64**, 155407(1)-155407(5).
41. Pivin, J. C.; Pippel, E.; Woltersdorf, J.; Avasthi, D. K.; Kumar, S. Structural transformations induced by swift heavy ions in polysiloxanes and polycarbosilanes, *Z. Metallkd* 2001, **92**, 712-716.
42. Srivastava, S.K.; Avasthi, D.K. & Pippel, E. Swift heavy ion induced formation of nanocolumns of C clusters in a Si based polymer, *Nanotechnology* 2006, **17**, 2518-2522.
43. Kumar, Amit.; Singh, F.; Khan, S. A.; Agarwal, D. C.; Tripathi, A.; Avasthi, D. K. & Pivin, J. C. Precipitation of semiconducting carbon nanoparticles in ion irradiated gels, *Nucl. Instr. And Meth. B* 2006, **244**, 23-26.
44. Tripathi, A.; Kumar, Amit.; Kabiraj, D.; Khan, S. A.; Baranwal, V. & Avasthi, D. K. SHI induced conducting tracks formation in C₆₀, *Nucl. Instr. and Meth. B* 2006, **244**, 15-18.
45. Kumar, Amit.; Avasthi, D. K.; Tripathi, A.; Kabiraj, D, Singh, F. & Pivin, J.C. Synthesis of confined electrically conducting carbon nanowires by heavy ion irradiation of fullerene thin film, *J. Appl. Phys.* 2007, **101**, 014308(1)-014308(5).
46. Prajakta, S.; Bhave, T.M.; Kanjilal, D.; Bhoraskar, S.V. Swift heavy ion induced growth of nanocrystalline silicon in silicon oxide, *J. Appl. Phys.* 2003, **93**, 3486-3489.
47. Rath, Shyama.; Kabiraj, D, Avasthi, D. K.; Tripathi, A.; Jain, K. P.; Kumar, Manoj.; Mavi, H. & Shukla, A. K. Evidence of nanostructure formation in Ge oxide by crystallization induced by swift heavy ion irradiation, *Nucl. Instr. And Meth. B* 2007, **263**, 419-423.
48. Biswas, A.; Avasthi, D.K, Fink, D.; Kanazov, J.; Schurmann, U.; Ding, S.J.; Aktas, O.C.; Saed, U.; Zaporojtchenko, V.; Faupel, F.; Gupta, R. & Kumar, N. Nanoparticle architecture in carbonaceous matrix upon swift heavy ion irradiation of polymer-metal nanocomposites, *Nucl. Instr. And Meth. B* 2004, **217**, 39-50.
49. Mishra, Y. K.; Avasthi, D. K.; Kulriya, P. K.; Singh, F.; Kabiraj, D, Tripathi, A, Pivin, J. C.; Bayer, I. S. & Biswas, Abhijit. Controlled growth of gold nanoparticles induced by ion irradiation: An *in situ* x-ray diffraction study, *Appl. Phys. Lett.* 2007, **90**, 73110(1)-73110(3).
50. Mishra, Y. K.; Singh, F.; Avasthi, D. K.; Pivin, J. C. & Malinowska, D. Synthesis of elongated Au nanoparticles in silica matrix by ion irradiation, *Appl. Phys. Lett.* 2007, **91**, 63103(1)-63103(3).
51. Mishra, Y.K.; Avasthi, D. K. & Pivin, J.C. Swift heavy ion induced dissolution of gold nanoparticles in silica matrix, *Rad. Effects and Defects in Solids* 2006, **162**, 207-213.
52. Singh, F.; Private communication.
53. Pivin, J.C.; Roger, G.; Garcia, M.A.; Singh, F. & Avasthi, D.K.; Nucleation and growth of Ag clusters in silicate glasses under ion irradiation, *Nucl. Instr. and Methods B* 2004, **215**, 373-384.
54. Singh, F.; Ph.D. thesis, Paris 2007.
55. Singh, F.; Mohapatra, S.; Stoquert, J.P.; Avasthi, D. K. & Pivin, J.C. Shape deformation of embedded metal nanoparticles by swift heavy ion irradiation, SHIM 2008 conference, July 2008, Lyon, France.
56. Balamurugan. B. & Mehta, B.R. Optical and structural properties of nanocrystalline copper oxide thin films prepared by activated reactive evaporation, *Thin Solid Films* 2001, **396**, 90-96.
57. Balamurugan. B.; Mehta, B.R.; Avasthi, D.K.; Singh, Fouran.; Arora, A.K.; Rajalakshmi, Raghavan, M, G.; Tyagi, A.K. & Shivaprasad, S.M. Modifying the nanocrystalline characteristics structure, size, and surface states of copper oxide thin films by high-energy heavy-ion irradiation, *J. of Appl. Phys.* 2002, **92**, 3304-3310.
58. Mohanta, D.; Nath, S.S.; Bordoloi, A.; Doloi, S.K.; Mishra, N.C. & Choudhury, A. Annual Report, NSC, page 2001-2002, 116.
59. Lotha, S.; Ingale, A.; Avasthi, D. K.; Mittal, V. K.; Mishra, S.; Rustagi, K. C.; Gupta, A.; Kulkarni, V. N. & Khating, D. T. Effect of heavy ion irradiation on C₆₀, *Solid State Communications* 1999, **111**, 55-60.
60. Bajwa, Navdeep.; Ingale, Alka.; Avasthi, D.K.; Kumar, Ravi.; Dharamvir, K. & Jindal, V.K. Swift heavy ion induced modification of C₆₀ thin films, *J. Appl. Phys.* 2003, **94**, 326-333.
61. Avasthi, D.K.; Assmann, W.; Nolte, H.; Mieskes, H. D.; Ghosh, S. & Mishra, N. C.; Transport of oxygen atoms mediated by electronic excitation, *Nucl. Instr. And Meth. B* 2000, **166/167**, 345-49.
62. Sharda, T.; Misra, D. S.; Avasthi, D. K. & Mehta, G.

- K. Dissociation kinetics of molecular hydrogen in a microwave plasma and its influence on the hydrogen content in diamond films, *Solid State Communications* 1996, **98**, 879-83.
63. Misra, Abha.; Tyagi, Pawan K.; Rai, Padmnabh, Misra, D.S, Ghatak, Jay.; Satyam, P.V. & Avasthi, D.K.; Reorientation of the crystalline planes in confined single crystal nickel nanorods induced by heavy ion irradiation, *Appl. Phys. Lett.* 2006, **89**, 091907(1)-091907(3).
 64. Misra, Abha.; Tyagi, Pawan K.; Rai, Padmnabh, Mohapatra, D.R.; Ghatak, Jay.; Satyam, P. V.; Avasthi, D.K. & Misra, D.S. Axial buckling and compressive behavior of nickel-encapsulated multiwalled carbon nanotubes, *Phys. Rev. B* 2007, **76**, 14108(1)-14108(5)
 65. Pradhan, A.K.; Roy, S.B.; Chaddah, P.; Kanjilal, D.; Chen, C. & Wanklyn, B.M.; Effects of 200-MeV Ag-ion irradiation on magnetization in a $Bi_2Sr_2CaCu_2O_{8+y}$ single crystal, *Phys. Rev. B* 1996, **53**, 2269-2272.
 66. Kumar, Ravi.; Samanta, S. B.; Arora, S. K.; Gupta, A.; Kanjilal, D.; Pinto, R. & Narlikar, A.V.; Study of columnar amorphization and structural symmetry changes produced by swift heavy ion irradiation in $YBa_2Cu_3O_{7-y}$ thin films using STM, *Solid State Communications* 1998, **106**, 805-810.
 67. Angadi, Basavaraj.; Jung, Y. S.; Choi, Won-Kook.; Kumar, Ravi.; Jeong, K.; Shin, S. W.; Lee, J. H.; Song, J. H.; Khan, M. Wasi. & Srivastava, J. P. Ferromagnetism in 200-MeV Ag^{+15} -ion-irradiated Co-implanted ZnO thin films, *Appl. Phys. Lett.* 2006, **88**, 142502 (1)-142502(3).
 68. Nakata, J.; Mechanism of low-temperature ($\leq 300^\circ\text{C}$) crystallization and amorphization for the amorphous Si layer on the crystalline Si substrate by high-energy heavy-ion beam irradiation, *Phys. Rev. B* 1991, **43**, 14643-14668.
 69. Viridi, G.S.; Pathak, B.C.; Avasthi, D.K. & Kanjilal, D.; Swift heavy ion-induced recrystallization of silicon-on-insulator (SOI) structures, *Nucl. Instr. and Meth. B* 2002, **187**, 189.
 70. Som, T.; Satapati, B.; Sinha, O.P.; Avasthi, D.K. & Kanjilal, D. Role of electronic and nuclear energy losses in swift heavy ion beam induced epitaxial crystallization of a buried Si_3N_4 layer, *Nucl. Instr. and Methods B* 2006, **245**, 255-259.
 71. Som, T.; Sinha, O. P.; Ghatak, J.; Satapati, B. & Kanjilal, D. MeV heavy ion induced recrystallization of buried silicon nitride layer: Role of energy loss processes, *J. Appl. Phys.* 2007, **101**, 34912 (1)-34912(4).
 72. Avasthi, D.K.; Ghosh, S.; Srivastava, S. K. & Assmann, W. Existence of transient temperature spike induced by SHI: evidence by ion beam analysis, *Nucl. Instr. and Meth. B* 2004, **219-220**, 206-214.

Contributor

Dr Devesh Kumar Avasthi (see page no. 362)